Mapping the coupled human and natural disturbance regimes of Europe's forests

Cornelius Senf[1,2] * and Rupert Seidl[1,2,3]

[1] Institute for Silviculture, University of Natural Resources and Life Sciences (BOKU), Vienna, Austria

[2] Ecosystem dynamics and forest management group, Technical University of Munich, Hans-Carl-von-Carlowitz-Platz 2, 85354 Freising, Germany

[3] Berchtesgaden National Park, Doktorberg 6, 83471, Berchtesgaden, Germany

*Corresponding author: Cornelius.senf@tum.de

Abstract: Forest disturbance shape ecosystem composition and structure, and changes in forest disturbances can have strong consequences for carbon storage and biodiversity. Yet we currently lack consistent quantitative data on Europe's forest disturbance regimes and their changes over time. Here we used satellite data to map three decades (1986-2016) of forest disturbances across continental Europe, covering 35 countries and a forest area of 210 Mill. ha at a spatial grain of 30 m, and analyzed the patterns and trends in disturbance size, frequency and severity. Between 1986 and 2016, 17% of Europe's forest area was disturbed by anthropogenic or natural causes, totaling to 25 Mill. individual disturbance patches with a mean patch size 1.09 ha (range between 1st and 99th percentile 0.18 – 10.10 ha). On average 0.52 (0.02 – 3.01) disturbances occurred per km² every year, removing on average 77% (22 – 100%) of the canopy. While spatial patterns of disturbance were highly variable, disturbance frequency consistently increased, and disturbance severity decreased since 1986. Both social and ecological factors are needed to explain the observed patterns and trends in forest disturbance. We thus conclude that in order to understand and manage the changes in Europe's forest disturbance regimes a coupled human and natural systems perspective is needed.

Keywords: Coupled Human and Environmental System; Disturbance regime; Remote sensing; Forest management; Resilience

Forests cover 33 % of Europe's total land area and provide important services to society, ranging from carbon sequestration to the filtration of water, protection of soil from erosion, and human infrastructure from natural hazards [1]. Europe's forests have expanded in recent decades [2] and accumulated substantial amounts of biomass due to intensive post-war reforestation programs, changes in management systems, and timber harvesting rates that remained below increment [3]. This success story of 20th century forestry in Europe, however, also has side effects, as the resultant changes in forest structure have – in combination with climate change – led to an episode of increasing forest disturbances in recent decades [4–7]. Increasing forest disturbances have the potential to erode Europe's carbon storage potential [8,9] and also impact other important services provided by Europe's forests [10,11]. Given a predicted increase in the demand for wood [1] and an expected future intensification of forest dieback under climate change [12], it is fundamental to increase the resilience of Europe's forests to changing disturbances [13–15].

Developing resilient management strategies requires a robust quantitative understanding of forest ecosystem dynamics [16]. In particular, it is essential to understand the disturbance regimes of Europe's forests [17]. Disturbance regimes characterize the cumulative effects of all disturbance events occurring in a given area and time period, and understanding them is fundamental to understanding the current state and future trajectories of forest ecosystems [18]. In Europe, however, forests have been utilized by humans for centuries, transforming species composition and structure [19–21], and consequently also the natural disturbance regimes of forests. In addition to this indirect effect, human land-use is directly disturbing forest canopies through timber harvesting, altering the rate and spatial patterns of forest disturbances compared to natural systems [22]. Human land-use also interacts with natural disturbances, e.g. by salvaging disturbed timber [23] and shortening early seral stages through planting [24]. More broadly, forest management alters biological legacies and landscape structure [23,25], with feedbacks on subsequent disturbances. Due to the intricate linkages

between natural and human processes driving forest disturbances in Europe, analyzing them in the context of coupled human and natural systems [26,27] is a promising approach. Given that relevant drivers of future changes in forest disturbance regimes are social-ecological (e.g., anthropogenic climate change, novel disturbances caused by the introduction of non-native disturbance agents, land-use change) applying such a perspective could considerably increase the inferential potential on current and future changes of forest dynamics cross Europe's forests.

Despite the widespread and long-lasting impacts of changing forest disturbances on forest ecosystems [10] little quantitatively information on disturbance regimes and their changes through time exist for Europe. We, for instance, do not know how disturbance size, frequency and severity (i.e., the main descriptors of disturbance regimes; [28]) are distributed throughout Europe. Furthermore, while recent studies indicate an increase in disturbance rates across Europe's natural and managed forests [4,6], it remains unknown whether this change is mainly driven by changes in disturbance frequency (i.e., more disturbance events) or disturbance size (i.e., larger individual disturbance patches). Likewise, our quantitative knowledge on changes in disturbance severity is scant, and it remains unclear whether disturbances in Europe have become more severe in recent decades (e.g., through increased burn severities; [29]) or whether recent changes in forest policy (e.g., the adoption of "close-to-nature" silviculture; [30]) have reduced disturbance severity [4].

Here, our aim was to map the patterns and trends of recent (1986-2016) forest disturbance regimes in Europe. Our specific research questions were: (I) What is the size, frequency and severity of forest disturbances across Europe's forests? And (II) How did size, frequency and severity of forest disturbances change over the past three decades? We address these first two questions by mapping forest disturbance occurrence and severity continuously for continental Europe (35 countries covering 210 Mill. ha of forest) at a spatial grain of 30 m. We subsequently analyze the disturbance regimes of Europe's forests in a coupled

87 human and natural systems framework, asking (III) how strongly patterns and trends in
88 disturbance size, frequency and severity are explained by variation in the natural template vs.
89 variation in forest policy. We address this third question by comparing the patterns and trends
90 in disturbance regime indicators among ecoregions (i.e., an aggregate proxy of the spatial
91 differences in the drivers of natural forest development) and countries (as the spatial entities
92 encapsulating the variation in forest policies in Europe [31]), hypothesizing that under a coupled
93 human and natural system perspective both social and ecological factors are needed to explain
94 patterns and trends in disturbance regimes across Europe's forests.

95 **Results**

96 We identified a total of 25 Mill. individual disturbance patches occurring across Europe
97 between 1986-2016, equaling a disturbed forest area of 4 Mill. ha or 17 % of Europe's forests
98 (Figure 1). The overall accuracy of our map was 92.5 %, with a disturbance commission error
99 of 14.6 % and a disturbance omission error of 32.8 %, but we refer the reader to
100 Supplementary Note 1 for further information on map accuracies. The average patch size of
101 forest disturbances in Europe was 1.09 ha, but the disturbance size distribution was highly
102 left-skewed (Figure 2 B). The median disturbance size was only 0.45 ha, with 78 % of the
103 disturbances being smaller than 1 ha and 99 % of the disturbances being smaller than 10 ha
104 (Supplement Table 2). The largest disturbance patch mapped across Europe was a 16,617 ha
105 large forest fire occurring in 2012 in southern Spain. The average disturbance frequency was
106 0.52 patches per km^2 per year (median of 0.37 patches per km^2), with highest frequencies
107 (highest 1 %) ranging from 3 to 31 patches per km^2 (Supplement Table 2). Disturbance
108 severity, that is a measure between 0 and 100 indicating the loss of canopy during disturbance
109 (see Figure 1C), ranged from 23 % to 100 %, with an average of 77 % of canopy loss within a
110 disturbed patch (median of 83 %; Supplement Table 2).

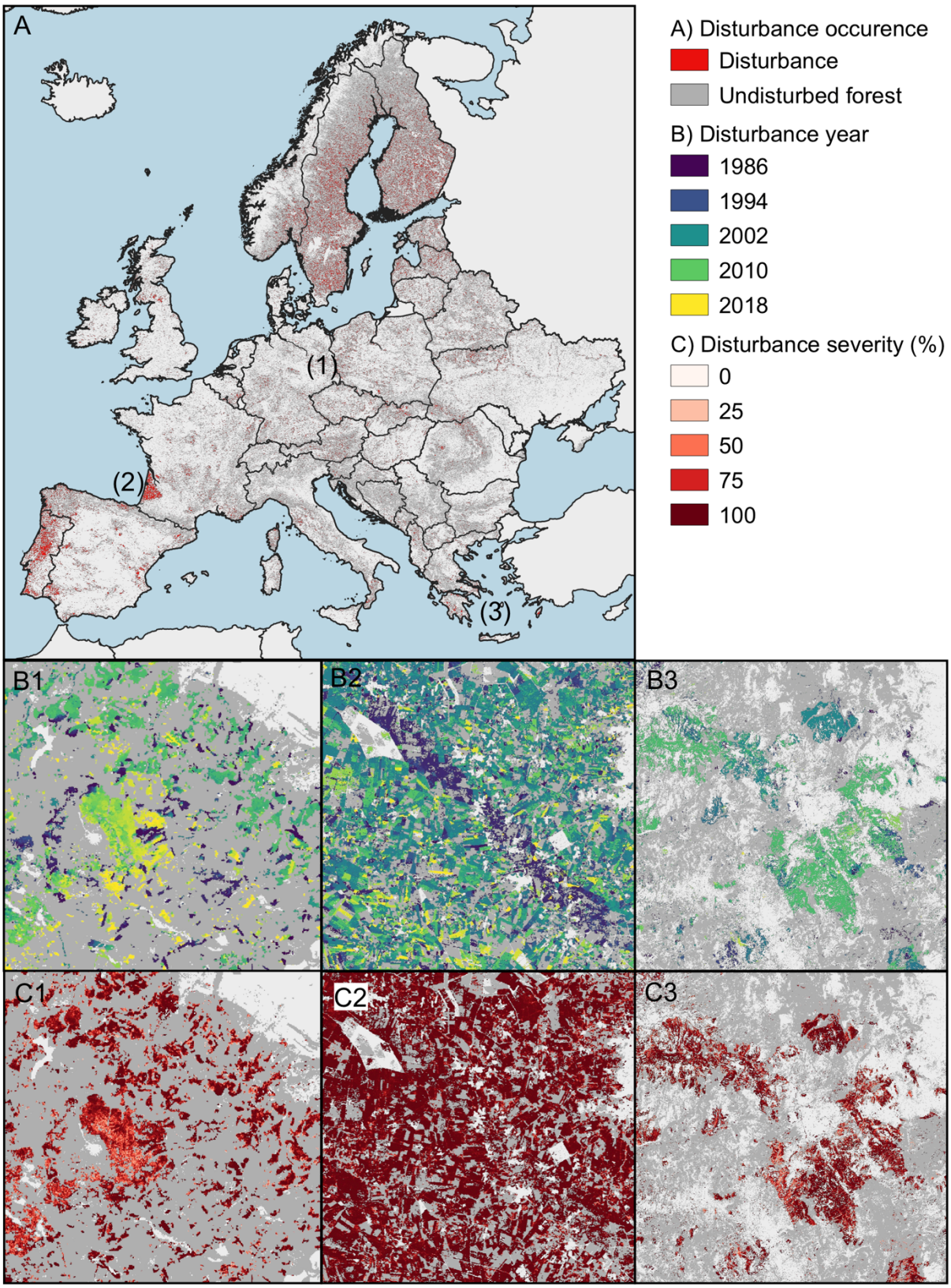

Fig. 1: Forest disturbances in Europe 1986-2016. Disturbance maps were derived from manually interpreting more than 30,000 Landsat images systematically distributed across Europe. Panel A shows the occurrence of disturbances across Europe. Panels B show the

disturbance year and panels C show the disturbance severity – a measure of canopy cover loss – for three selected areas: (1) Bark beetle outbreak of varying severity in and around Harz National Park (Germany); (2) wind disturbance in an intensively managed plantation forest in the Landes of Gascony (France) with very high disturbance severities; and (3) fire disturbances on the Peloponnese peninsula (Greece), with variable burn-severities.

Spatial variability in the size, frequency and severity of forest disturbances is high across Europe (Figure 2 A). Disturbance patches are generally larger in Northern and Southern Europe compared to Central Europe. Also, Eastern Europe has larger disturbance patches compared to Western Europe (Figure 2 A). Above-average disturbance frequencies were found in Central Europe, the hemi-boreal zone, parts of France and the Iberian Peninsula (Figure 2 A). The highest disturbance frequencies (i.e., above 3 patches per km^2) occurred almost exclusively in Portugal. Disturbance severity was more evenly distributed than the other two disturbance regime indicators (Figure 2 A), with a tendency towards higher severities in the Atlantic forests of Ireland and the United Kingdom, the Iberian Peninsula, the Po-Valley, and the Pannonian Basin. In contrast, low disturbance severities were recorded for South-Eastern Europe along the Dinaric mountain range, as well as in the Apennine mountains of Italy.

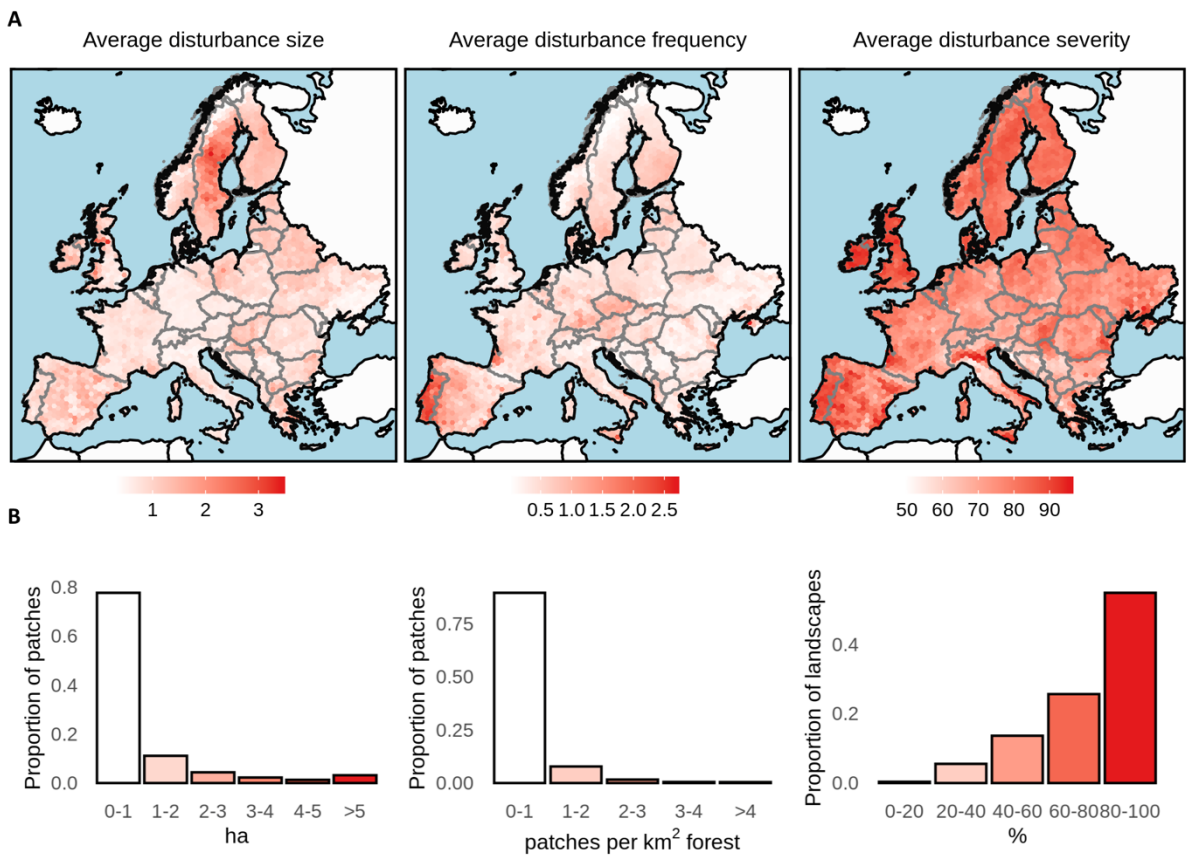

Fig. 2: (A) Maps of average disturbance size, frequency and severity calculated for hexagons on a 50 km grid across continental Europe. (B) Distribution of disturbance size, frequency and severity across Europe.

Disturbance regimes changed profoundly between 1986 and 2016, with 65 % of Europe's forests experiencing an increase in disturbance size, and 74 % an increase in disturbance frequency (Figure 3 B). Hot spots of increasing disturbance size were in the Baltic states, the United Kingdom, Ireland, and Italy (Figure 3 A), whereas trends were largely negative in Eastern Germany, western Poland and southeastern Europe (Figure 3 A). Hot spots of increasing disturbance frequency were located in Central and Eastern Europe (Figure 3), whereas negative trends in disturbance frequency were recorded for Belarus, western Europe, and northern Scandinavia (Figure 3 A). Disturbance severity decreased in

85 % of the European forest area (Figure 3), with particularly strong trends in Central and Southeastern Europe.

While the mean disturbance size generally increased across Europe (Figure 3) the median disturbance size was more stable (no change in median disturbance size in 81 % of European forests; Supplementary Table 3). Hence, changes in disturbance size were driven by a widening of the disturbance size distribution, with approximately 50 % of Europe's forests showing an increase in large disturbance patches (i.e., in the 75% quantile and maximum of the disturbance patch size distribution; Supplement Table 3). Overall, changes in disturbance frequency explained 71 % of the variability in changing disturbance rates (i.e., the trend in the annual percent of forest area disturbed), whereas changes in disturbance size only accounted for 24 % (see Supplementary Figure 8). Thus, changes in disturbance rates are primarily driven by changes in disturbance frequency, and not disturbance size, in Europe's forests.

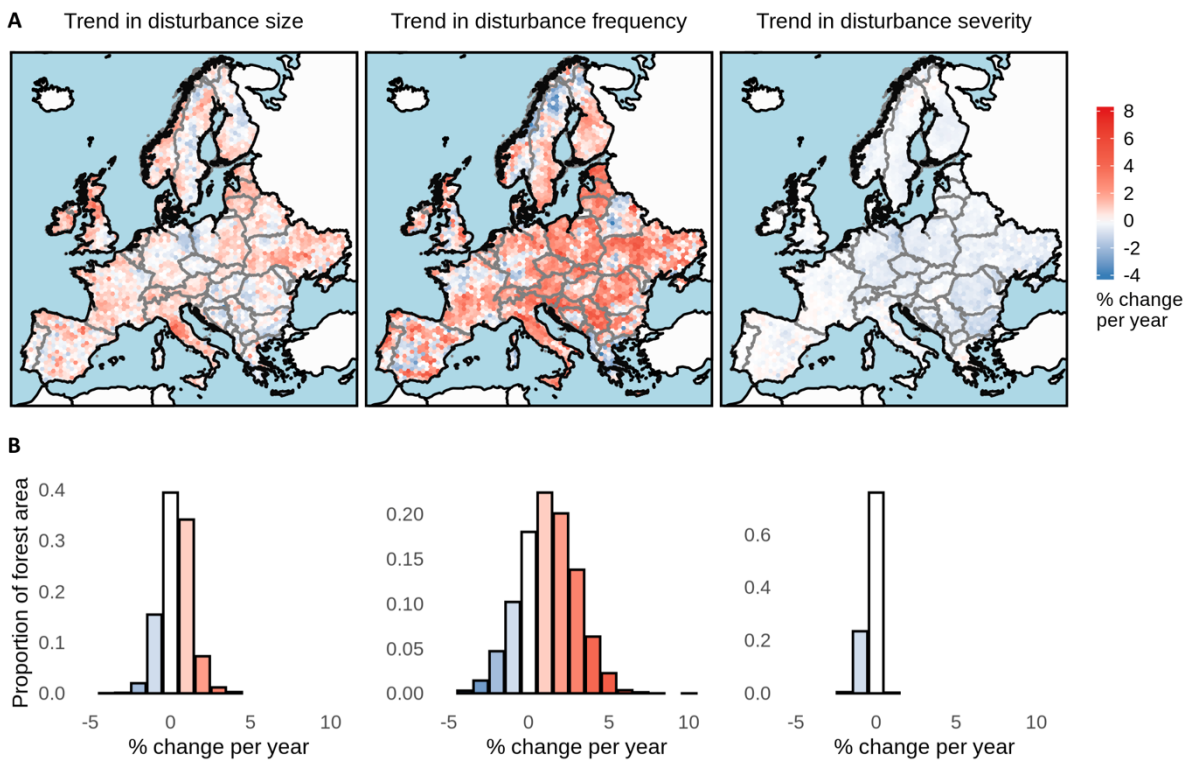

Fig. 3: (A) Maps of trends in disturbance size, frequency and severity calculated at a 50 km hexagon grid across continental Europe. (B) Distribution of forest area among trend classes.

Spatial variability in all three disturbance regime indicators varied significantly with ecoregion (i.e., a coarse filter proxy of spatial differences in the drivers of natural forest development), and ecoregions alone explained 15, 28 and 39 % of the continental-scale spatial variation in disturbance size, frequency and severity, respectively (Table 1). Including within-ecoregion variability by country (i.e., a coarse filter proxy for differences in forest policy and management) further increased the variance explained by 16, 24 and 16 percentage points, respectively (Table 1).

Table 1: Variance explained by ecoregions and countries nested within ecoregions derived from linear mixed effect models testing for differences in averages and trends in disturbance size, frequency and severity measured across 3,240 50 km^2 hexagons. Also shown is the amount of variance explained by random variation among years (for averages), as well as the residual variance (i.e., variance not explained by the two coarse filter variables used here).

Indicator	Variance explained			Residual variance
	Ecoregions	Ecoregions/countries	Year	
Average				
Mean size (log)	0.15	0.16	0.01	0.67
Frequency (log)	0.28	0.24	0.03	0.45
Severity	0.39	0.16	0.07	0.37
Trend				
Mean size	0.12	0.11	-	0.77
Frequency	0.09	0.24	-	0.67
Severity	0.19	0.14	-	0.68

Trends in size and severity were also determined by a combination of ecoregions and policy differences within ecoregions, with the two factors explaining roughly equal parts of the spatial variation in disturbances trends (Table 1). For changes in frequency ecoregion alone was a poor predictor, whereas country explained 24 % of the variance in frequency trends (Table 2). Hence, while the ecological template determines the general spatial pattern of the disturbance regimes in Europe, human activity modulates this pattern considerably (for

183 estimates see Supplementary Figure S9, S10), underlining the coupled human and natural
184 nature of forest disturbances in Europe.

185 **Discussion**

186 We here provide the first quantitative characterization of Europe's forest disturbance regimes,
187 highlighting the wide variability in disturbance sizes, frequencies and severities prevailing
188 across the European continent. We show that this variability is determined by the combined
189 effects of natural processes (i.e., variation in climate and soil, resulting in different forest
190 development trajectories) and human activity (i.e., variation in forest policy, resulting in
191 different management regimes). Differences in forest policy can be large even among
192 neighboring countries in Europe, especially among countries of variable socio-political
193 histories (e.g., the iron curtain dividing the continent into two geopolitical spheres). These
194 differences in forest policy result in different management intensities and silvicultural
195 practices [31] and variable land use legacies [21]. For example, spatial patterns of timber
196 extraction can vary widely between countries, resulting in contrasting disturbance sizes and
197 frequencies within ecoregions (Supplementary Figure S11). Another example for the impact
198 of forest policy on disturbance regimes is the varying share of plantation forests with non-
199 native tree species [1], such as *Eucalyptus* sp. in Portugal or Black locust (*Robinia*
200 *pseudoacacia*) in Hungary (Supplementary Figure S12). Human activity thus has a profound
201 impact on the forest disturbance regimes of Europe, on the one hand altering disturbance
202 regimes directly via timber harvesting, and on the other hand indirectly modifying disturbance
203 processes through changing species composition and forest structure. Our results hence
204 support the hypothesis that the European forest disturbance regime is a coupled human and
205 natural system, driven by the complex interplay between social and ecological forces.

206 The disturbance regimes of Europe's forests are changing profoundly. We here show
207 that the previously reported increase in disturbance activity [4,6,7] is primarily an effect of

increasing disturbance frequency, while disturbance patch size distributions are becoming more variable and disturbance severities are decreasing. Variation in forest policy was a more important predictor of changing disturbance frequencies than the variation in the natural template, suggesting human resource use as a major driver of change [1,4,7,32]. In contrast, the widening of the patch size distribution likely results from the combined effects of management changes (towards smaller intervention sizes) and increased natural disturbance activity (resulting in large areas of canopy removal). The same developments also result in decreasing disturbance severity at the continental scale, with management systems being optimized to reduce impact [33] and natural disturbance events being frequently characterized by mixed severities [34]. We conclude that recent trends in Europe's forest disturbance regimes are strongly driven by the interaction of social and ecological forces, with human resource use feedbacking to the natural system and *vice versa* (Figure 4).

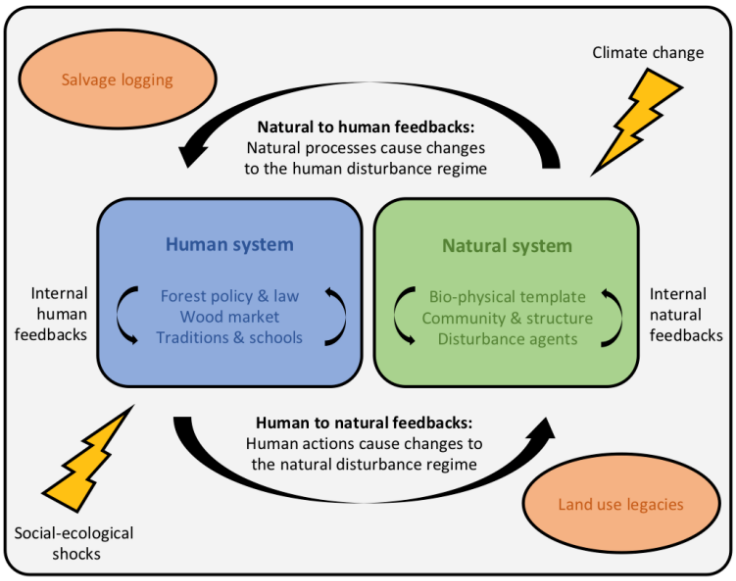

Fig. 4: Europe's disturbance regimes as coupled human and natural system.

Our results have important implications for the future of Europe's forests. First, by characterizing the recent disturbance regimes of Europe we provide a baseline to assess future

226 changes. This is important as disturbances are expected to change considerably in the coming
227 decades [22,35], yet a sound quantitative baseline for quantifying these changes has been missing
228 to date. Second, we highlight that both socio-ecological shocks (such as reforestation waves
229 after the Second World War [3] or the collapse of the Soviet Union [36]) and changes in the
230 biophysical environment (such as climate change) drive changes in forest disturbance regimes
231 (Figure 4). This has important consequences for managing the resultant negative
232 consequences of increasing disturbances on ecosystem service provisioning [10]. In particular,
233 our analyses suggest that efforts focusing on both the mitigation of climate change and the
234 compensation of increasing canopy openings in forest policy and management are needed to
235 bend the curve and stabilize forest canopy turnover at sustainable rates [37]. A further focus
236 should be on steering the intricate social-ecological interactions driving disturbance regimes
237 towards dampening feedbacks (Figure 4). For instance, management should focus on creating
238 land use legacies that reduce the propensity of natural disturbances in the future [28,38], which
239 will reduce the need for management techniques that cause harm to important ecosystem
240 services and biodiversity (i.e., salvage logging) [25,39]. Overall, we suggest that acknowledging
241 complex social-ecological interactions is elementary for managing Europe's forests and key
242 to creating resilient systems that will sustain important functions and services under an
243 uncertain future.
244

Materials and Methods

Reference data

Acquiring consistent reference data across large areas – such as continental Europe – is challenging and we therefore make use of manual interpretation of satellite data, serving as valuable alternative to field-based data [40]. Manual interpretation of satellite data for calibrating and validating Landsat-based forest change maps is a well-established approach and has been used in numerous studies previously [41–44]. In essence, an interpreter inspects the temporal profile of a Landsat pixel and, with the help of Landsat image chips and very high-resolution imagery available in Google Earth, makes a well-informed call whether the trajectory represents a stable forest or a forest experiencing a mortality event [45]. We here used a previously established set of 19,996 interpreted Landsat pixels [4,7]. The initial sample was drawn at random within forests of Europe, with samples stratified by country. Yet, as interpreters might declare a plot as no-forest during interpretation (caused by errors in the automatically generated forest mask), the realized sample size slightly varied (Table S1). Please note that samples for six Central European countries stem from another study using the same image interpretation approach but have higher sampling densities. The response design followed well-documented protocols developed and published previously [4]. Manual interpretation was done by a total of nine interpreters using established software tools [45], and the data is freely accessible under following repository:
https://doi.org/10.5281/zenodo.3561925

The reference sample set only consisted of forest pixels and there was thus need for substituting the sample with non-forest reference pixels. We therefore drew a country-stratified sample of non-forest pixels using a Landsat-based land cover map from [46]. Each countries sample size was chosen to match the forest proportion of the respective country (based on data from the FAOSTATS database), that is the total sample of each country equaled a random sample across its terrestrial forested and non-forested land surface (see

Table S1). In total we drew 46,461 non-forest reference pixel that, paired with the 19,996 forest reference pixels manually interpreted, totaled to 66,457 reference pixels used for calibration and validation. From the full reference sample, we randomly drew a sub-sample of 5,000 pixels for map validation, and the remaining 61,457 pixels were used for model calibration. The validation sub-sample was drawn proportionally to the size of each country to ensure a consistent and unbiased estimation of map accuracies for the final European map product.

Mapping disturbances

At the core of our mapping workflow we rely on an established time-series segmentation approach called LandTrendr [47], implemented in the high-performance cloud-computing environment Google Earth Engine [48]. In essence, LandTrendr segments annual Landsat pixel time series into linear features from which a set of metrics can be extracted. We here do not provide details on the underlying LandTrendr routines but focus on the salient details of our mapping workflow (please see Figure S2 for a graphical outline of our mapping workflow). The workflow was based on code published in Kennedy et al. [48].

In a first step we screened all available Tier 1 Landsat 4, 5, 7 and 8 images in the United States Geological Survey archive. Tier 1 images are delivered as ready-to-use surface reflectance images including a cloud mask, yet we used coefficients from Roy et al. [49] to spectrally align the varying sensor types used onboard Landsat 4/5 (Thematic Mapper), Landsat 7 (Enhanced Thematic Mapper Plus), and Landsat 8 (Operational Land Imager). After spectral alignment we filtered all available images for summer-season acquisition dates (1st of June to 30th September) and built annual medoid composites following Flood [50].

Second, we ran LandTrendr for two spectral bands (shortwave infrared I and II) and two spectral indices commonly used for forest disturbance and mortality mapping [43,44,51–53]: The Tasseled Cap wetness (TCW) and the Normalized Burn Ration (NBR). We used a

standard parameter set for LandTrendr with no filtering or thresholding and thus allowing for maximum sensitivity in detecting changes (i.e., allowing for a high commission error).

Third, we extracted the greatest change segment from each pixel's LandTrendr fit to both spectral bands and both spectral indices. From the greatest change segment we derived a set of three metrics describing the magnitude, duration and rate of change [51]; as well as a measure of the signal-to-noise ratio described in Cohen et al. [52]. We further derived the spectral band/index value prior to, and the rate of change following the greatest change segment. Similar metrics as the ones used here have been applied also in many previous studies mapping forest cover changes [42,44,53].

Fourth, we used the set of metrics derived from the greatest change segment for the two spectral bands and the two spectral indices, the calibration data outlined in the previous section, and random forest classification [54] to classify each pixel into either no-forest, undisturbed forest or disturbed forest (i.e., at least one disturbance event during the study period). This last step filtered out commission errors by LandTrendr and thus greatly improves mapping accuracy compared to purely automatic algorithms [55]. Yet, we experienced difficulties in correctly separating forest and no-forest areas solely based on LandTrendr outputs. This was due to high spectral changes in agricultural areas, which were identified as disturbances by LandTrendr. To tackle this problem, we added a three-year Tasseled Cap Brightness, Greenness and Wetness median composite centered on 1985 and 2018, respectively, to the classification stack. The additional six bands delivered more detailed spectral information on stable forest and no-forest pixels. Finally, we applied the trained random forest model to the full classification stack (i.e., LandTrendr metrics from the two spectral bands and two spectral indices plus the Tasseled Cap composite from 1985 and 2018) to consistently map the categories no forest, undisturbed forest and forest disturbances across continental Europe. We validated the final map using the validation sub-sample described in

the previous section. We derived a confusion matrix and report overall accuracy, errors of commission and errors of omission following best-practice recommendations given in [40].

Fifth, while the thus derived map indicates that a mortality event has happened, they do not indicate when the mortality event happened. We therefore calculated the disturbance onset year (i.e., the year of the greatest spectral change) from all spectral bands and spectral indices using a majority vote. If there was a tie (e.g., all four bands/indices indicated a different year), we reverted to the median value. To validate this processing step, we compared the year assigned from LandTrendr to the manually interpreted year of disturbance for the 19,996 forest reference plots.

Spatial filtering

The last step in creating disturbance maps for continental Europe was to apply a set of spatial filters for smoothing the resulting disturbance maps and enhancing spatial pattern analysis. We first set a minimum mapping unit of two 30 × 30 m pixels (i.e., 0.18 ha) and removed all patches smaller than the minimum mapping unit. In a second filtering step, we identified all annual patches smaller than the minimum mapping unit and assigned them to the year of the surrounding pixels, thus smoothing the definition of patches (see Figure S3). In a final filtering step, we removed holes within mortality patches smaller than the minimum mapping unit by filling them with the year of the surrounding pixels. While the spatial filtering was done to improve the spatial analysis described in the following section, we note that the filtering was applied after the accuracy assessment. The accuracy assessment thus reports the raw classification performance without additional filtering.

Characterizing disturbance regimes and their changes

From the annual forest disturbance maps we calculated three disturbance regime indicators based on Turner [17] and Johnstone et al. [28]: disturbance size, frequency and severity. Disturbance size and severity were first calculated at the patch level and then aggregated to the landscape level, while disturbance frequency was calculated at the landscape level

347 directly. Patch size is the number of disturbed pixels for each individual patch (patches were
348 defined annually using a rook-contiguity) multiplied by pixel size (0.09 ha). For calculating
349 disturbance frequency, we sub-divided the total study area into a 50 * 50 km hexagon grid
350 (here representing the landscape scale), totaling to 3,240 hexagons across Europe's land area.
351 We chose hexagons over squares, as hexagons minimize the spatial difference to the more
352 complex border of countries and ecoregions used in later analysis. For each hexagon, we then
353 counted the number of individual patches per year and divided this number by the total forest
354 area within the hexagon, yielding a measure of the number of patches per km^2 forest area per
355 year as in indicator of disturbance frequency.

356 For quantifying disturbance severity, we made use of the spectral change magnitude
357 provided by the LandTrendr analysis. The spectral change magnitude during disturbance is
358 well correlated with changes in vegetation cover [51,56–59]. Consequently, we here use it as
359 measure of canopy cover change within a disturbed patch. To combine the spectral change
360 magnitude from all four spectral bands/indices into one index of canopy cover change we
361 used logistic regression to predict the occurrence of stand-replacing disturbances from the
362 four spectral change magnitudes. Data on stand replacing disturbances was generated from
363 the reference sample by analyzing the manually interpreted land cover after a disturbance
364 segment. If the land cover switched to non-treed following a disturbance segment (e.g., after
365 clear-cut harvest or high intensity fire), the disturbance is assigned as stand-replacing. If the
366 land cover remains treed following a disturbance segment (e.g., following a thinning
367 operation or a low intensity windthrow), the disturbance is classified as non-stand-replacing.
368 The method is based on Senf et al. [4] who showed that visual interpretation of post-disturbance
369 land cover is an accurate measure for separating stand-replacing from non-stand-replacing
370 disturbances. By predicting the occurrence of stand-replacing disturbances (i.e., complete
371 removal of the canopy), we scale the spectral change magnitudes to a value between 0 and 1
372 (or 0 % and 100%), where 1 (or 100 %) indicates complete canopy loss. We validated this

measure of disturbance severity by separating stand-replacing and non-stand-replacing disturbances solely based on disturbance severity, expecting a high discriminatory power in separating the different disturbance types.

For spatially visualizing disturbance size, frequency and severity, as well as for calculating and visualizing trends, we finally aggregated the patch-based metrics (i.e., disturbance size and severity) to the landscape level (i.e., the hexagon) by calculating the arithmetic mean. We report the mean over the median as it is sensitive to changes in both the central tendency and the spread of the distribution, but we also report other statistics in the Supplement. Trends in disturbance size, frequency and severity were quantified using a non-parametric Theil–Sen estimator, which is a non-parametric measure of monotonic trends in time series insensitive to outliers [60].

Statistical analysis of differences between ecoregions and countries

We used linear mixed effect models (LMM) to test for differences in averages and trends in disturbance size, frequency and severity among ecoregions and countries nested within ecoregions. Both ecoregions and countries nested within ecoregions were modelled as random effects, assuming the individual averages and trends emerging from a common underlying distribution [61]. For the average modes we also considered years as random effect. From the fitted LMMs we calculated the variance partition coefficient, that is the amount of variance explained by ecoregions, countries within ecoregions, and the residual variance within countries nested within ecoregions (i.e., variance not explained).

394 **References**

395 1. Forest Europe. *State of Europe's forests 2015*. (2015).

396 2. Fuchs, R., Herold, M., Verburg, P. H., Clevers, J. G. P. W. & Eberle, J. Gross changes
397 in reconstructions of historic land cover/use for Europe between 1900 and 2010. *Global*
398 *Change Biology* **21**, 299–313 (2015).

399 3. Ciais, P. *et al.* Carbon accumulation in European forests. *Nature Geoscience* **1**, 425–
400 429 (2008).

401 4. Senf, C. *et al.* Canopy mortality has doubled across Europe's temperate forests in the
402 last three decades. *Nature Communications* **9**, 4978 (2018).

403 5. Seidl, R., Schelhaas, M.-J. & Lexer, M. J. Unraveling the drivers of intensifying forest
404 disturbance regimes in Europe. *Global Change Biology* **17**, 2842–2852 (2011).

405 6. Senf, C. & Seidl, R. Natural disturbances are spatially diverse but temporally
406 synchronized across temperate forest landscapes in Europe. *Global Change Biology* **24**,
407 1201–1211 (2018).

408 7. Senf, C., Sebald, J. & Seidl, R. Increasing canopy mortality challenges the future of
409 Europe's forests. (In revision).

410 8. Nabuurs, G.-J. *et al.* First signs of carbon sink saturation in European forest biomass.
411 *Nature Climate Change* **3**, 792–796 (2013).

412 9. Seidl, R., Schelhaas, M. J., Rammer, W. & Verkerk, P. J. Increasing forest
413 disturbances in Europe and their impact on carbon storage. *Nature Climate Change* **4**, 806–
414 810 (2014).

415 10. Thom, D. & Seidl, R. Natural disturbance impacts on ecosystem services and
416 biodiversity in temperate and boreal forests. *Biological Reviews* **91**, 760–81 (2016).

417 11. Lindner, M. *et al.* Climate change impacts, adaptive capacity, and vulnerability of
418 European forest ecosystems. *Forest Ecology and Management* **259**, 698–709 (2010).

419 12. Allen, C. D. *et al.* A global overview of drought and heat-induced tree mortality

420 reveals emerging climate change risks for forests. *Forest Ecology and Management* **259**, 660–
421 684 (2010).
422 13. Trumbore, S., Brando, P. & Hartmann, H. Forest health and global change. *Science*
423 **349**, 814–8 (2015).
424 14. Millar, C. I., Stephenson, N. L. & Stephens, S. L. CLIMATE CHANGE AND
425 FORESTS OF THE FUTURE: MANAGING IN THE FACE OF UNCERTAINTY.
426 *Ecological Applications* **17**, 2145–2151 (2007).
427 15. Seidl, R. The Shape of Ecosystem Management to Come: Anticipating Risks and
428 Fostering Resilience. *BioScience* **64**, 1159–1169 (2014).
429 16. Bengtsson, J., Nilsson, S. G., Franc, A. & Menozzi, P. Biodiversity, disturbances,
430 ecosystem function and management of European forests. *Forest Ecology and Management*
431 **132**, 39–50 (2000).
432 17. Turner, M. G. Disturbance and landscape dynamics in a changing world. *Ecology* **91**,
433 2833–49 (2010).
434 18. Asner, G. P. Geography of forest disturbance. *Proceedings of the National Academy of*
435 *Sciences of the United States of America* **110**, 3711–2 (2013).
436 19. Bebi, P. *et al.* Changes of forest cover and disturbance regimes in the mountain forests
437 of the Alps. *Forest Ecology and Management* **388**, 43–56 (2017).
438 20. Kulakowski, D., Bebi, P. & Rixen, C. The interacting effects of land use change,
439 climate change and suppression of natural disturbances on landscape forest structure in the
440 Swiss Alps. *Oikos* **120**, 216–225 (2011).
441 21. Munteanu, C. *et al.* Legacies of 19th century land use shape contemporary forest
442 cover. *Global Environmental Change-Human and Policy Dimensions* **34**, 83–94 (2015).
443 22. Sommerfeld, A. *et al.* Patterns and drivers of recent disturbances across the temeprate
444 forest biome. *Nature Communications* **9**, (2018).
445 23. Lindenmayer, D. B. *et al.* Salvage harvesting policies after natural disturbance.

Science **303**, 1303 (2004).

24. Senf, C., Müller & Seidl, R. Post-disturbance recovery of forest cover and tree height differ with management in Central Europe. *Landscape Ecology* (2019).

25. Thorn, S. *et al.* Impacts of salvage logging on biodiversity: A meta-analysis. *Journal of Applied Ecology* **55**, 279–289 (2018).

26. Jianguo Liu *et al.* Coupled Human and Natural Systems. *AMBIO: A Journal of the Human Environment* **36**, 639–649 (2007).

27. Liu, J. *et al.* Complexity of Coupled Human and Natural Systems. *Science* **317**, 1513–1516 (2007).

28. Johnstone, J. F. *et al.* Changing disturbance regimes, ecological memory, and forest resilience. *Frontiers in Ecology and the Environment* **14**, 369–378 (2016).

29. Stephens, S. L. *et al.* Temperate and boreal forest mega-fires: characteristics and challenges. *Frontiers in Ecology and the Environment* **12**, 115–122 (2014).

30. Brang, P. *et al.* Suitability of close-to-nature silviculture for adapting temperate European forests to climate change. *Forestry* **87**, 492–503 (2014).

31. Levers, C. *et al.* Drivers of forest harvesting intensity patterns in Europe. *Forest Ecology and Management* **315**, 160–172 (2014).

32. Curtis, P. G., Slay, C. M., Harris, N. L., Tyukavina, A. & Hansen, M. C. Classifying drivers of global forest loss. *Science* **361**, 1108–1111 (2018).

33. Mori, A. S. & Kitagawa, R. Retention forestry as a major paradigm for safeguarding forest biodiversity in productive landscapes: A global meta-analysis. *Biological Conservation* **175**, 65–73 (2014).

34. Meigs, G. W. *et al.* More ways than one: Mixed-severity disturbance regimes foster structural complexity via multiple developmental pathways. *Forest Ecology and Management* **406**, 410–426 (2017).

35. Dale, V. H. *et al.* Climate Change and Forest Disturbances. *BioScience* **51**, 723–734

(2001).

36. Kuemmerle, T. *et al.* Post-Soviet farmland abandonment, forest recovery, and carbon sequestration in western Ukraine. *Global Change Biology* **17**, 1335–1349 (2011).

37. Lindenmayer, D., Messier, C. & Sato, C. Avoiding ecosystem collapse in managed forest ecosystems. *Frontiers in Ecology and the Environment* **14**, 561–568 (2016).

38. Seidl, R., Donato, D. C., Raffa, K. F. & Turner, M. G. Spatial variability in tree regeneration after wildfire delays and dampens future bark beetle outbreaks. *Proc Natl Acad Sci U S A* **113**, 13075–13080 (2016).

39. Dobor, L. *et al.* Is salvage logging effectively dampening bark beetle outbreaks and preserving forest carbon stocks? *Journal of Applied Ecology* **n/a**,.

40. Olofsson, P. *et al.* Good practices for estimating area and assessing accuracy of land change. *Remote Sensing of Environment* **148**, 42–57 (2014).

41. Potapov, P. V. *et al.* Eastern Europe's forest cover dynamics from 1985 to 2012 quantified from the full Landsat archive. *Remote Sensing of Environment* **159**, 28–43 (2015).

42. Senf, C., Pflugmacher, D., Hostert, P. & Seidl, R. Using Landsat time series for characterizing forest disturbance dynamics in the coupled human and natural systems of Central Europe. *ISPRS J Photogramm Remote Sens* **130**, 453–463 (2017).

43. Kennedy, R. E. *et al.* Spatial and temporal patterns of forest disturbance and regrowth within the area of the Northwest Forest Plan. *Remote Sensing of Environment* **122**, 117–133 (2012).

44. Hermosilla, T., Wulder, M. A., White, J. C., Coops, N. C. & Hobart, G. W. An integrated Landsat time series protocol for change detection and generation of annual gap-free surface reflectance composites. *Remote Sensing of Environment* **158**, 220–234 (2015).

45. Cohen, W. B., Yang, Z. & Kennedy, R. Detecting trends in forest disturbance and recovery using yearly Landsat time series: 2. TimeSync — Tools for calibration and validation. *Remote Sensing of Environment* **114**, 2911–2924 (2010).

46. Pflugmacher, D., Rabe, A., Peters, M. & Hostert, P. Mapping pan-European land cover using Landsat spectral-temporal metrics and the European LUCAS survey. *Remote Sensing of Environment* (2018).

47. Kennedy, R. E., Yang, Z. & Cohen, W. B. Detecting trends in forest disturbance and recovery using yearly Landsat time series: 1. LandTrendr — Temporal segmentation algorithms. *Remote Sensing of Environment* **114**, 2897–2910 (2010).

48. Kennedy, R. *et al.* Implementation of the LandTrendr Algorithm on Google Earth Engine. *Remote Sensing* **10**, (2018).

49. Roy, D. P. *et al.* Characterization of Landsat-7 to Landsat-8 reflective wavelength and normalized difference vegetation index continuity. *Remote Sensing of Environment* **185**, 57–70 (2016).

50. Flood, N. Seasonal Composite Landsat TM/ETM+ Images Using the Medoid (a Multi-Dimensional Median). *Remote Sensing* **5**, 6481–6500 (2013).

51. Pflugmacher, D., Cohen, W. B. & E. Kennedy, R. Using Landsat-derived disturbance history (1972–2010) to predict current forest structure. *Remote Sensing of Environment* **122**, 146–165 (2012).

52. Cohen, W. B., Yang, Z., Healey, S. P., Kennedy, R. E. & Gorelick, N. A LandTrendr multispectral ensemble for forest disturbance detection. *Remote Sensing of Environment* **205**, 131–140 (2018).

53. Senf, C., Pflugmacher, D., Wulder, M. A. & Hostert, P. Characterizing spectral–temporal patterns of defoliator and bark beetle disturbances using Landsat time series. *Remote Sensing of Environment* **170**, 166–177 (2015).

54. Breiman, L. Random Forests. *Machine Learning* **45**, 5–32 (2001).

55. Cohen, W. *et al.* How Similar Are Forest Disturbance Maps Derived from Different Landsat Time Series Algorithms? *Forests* **8**, 98 (2017).

56. Bright, B. C., Hudak, A. T., Kennedy, R. E. & Meddens, A. J. H. Landsat Time Series

and Lidar as Predictors of Live and Dead Basal Area Across Five Bark Beetle-Affected Forests. *IEEE Journal of Selected Topics in Applied Earth Observations and Remote Sensing* **7**, 3440–3452 (2014).

57. Zald, H. S. J. *et al.* Integrating Landsat pixel composites and change metrics with lidar plots to predictively map forest structure and aboveground biomass in Saskatchewan, Canada. *Remote Sensing of Environment* **176**, 188–201 (2016).

58. Meigs, G. W., Kennedy, R. E., Gray, A. N. & Gregory, M. J. Spatiotemporal dynamics of recent mountain pine beetle and western spruce budworm outbreaks across the Pacific Northwest Region, USA. *Forest Ecology and Management* **339**, 71–86 (2015).

59. Meddens, A. J. H. & Hicke, J. A. Spatial and temporal patterns of Landsat-based detection of tree mortality caused by a mountain pine beetle outbreak in Colorado, USA. *Forest Ecology and Management* **322**, 78–88 (2014).

60. Wilcox, R. R. *Fundamentals of modern statistical methods: Substantially improving power and accuracy*. (Springer, 2010).

61. Gelman, A. Multilevel (Hierarchical) Modeling: What It Can and Cannot Do. *Technometrics* **48**, 432–435 (2006).

Acknowledgements

C. Senf acknowledges funding from the Austrian Science Fund (FWF) Lise-Meitner Program (Nr. M2652). R. Seidl acknowledges funding from FWF START grant Y895-B25. We thank Justin Brasten (Oregon State University) for making the code of LandTrendr open source, which greatly helped in implementing this research.

Author contribution

CS and RS designed the research; CS performed all computations and analyses; CS wrote the manuscript with input from RS.

Data availability

All maps presented in this research paper will be made publicly available after peer-review.

Code availability

The code used for processing the Landsat data is available at https://github.com/eMapR/LT-GEE. The research code used for creating the maps will be made available after peer-review.